Tribol Lett (2016) 61:17
DOI 10.1007/s11249-015-0631-1

ORIGINAL PAPER

Insigths into the Tribochemistry of Silicon-doped Carbon-Based Films by Ab Initio Analysis of Water–Surface Interactions

Seiji Kajita[1,2] · **M. C. Righi**[2]

Received: 3 November 2015 / Accepted: 27 November 2015 / Published online: 19 January 2016

Abstract Diamond and diamond-like carbon are used as coating materials for numerous applications, ranging from biomedicine to tribology. Recently, it has been shown that the hydrophilicity of the carbon films can be enhanced by silicon doping, which highly improves their biocompatibility and frictional performances. Despite the relevance of these properties for applications, a microscopic understanding on the effects of silicon is still lacking. Here, we apply ab initio calculations to study the interaction of water molecules with Si-incorporating C(001) surfaces. We find that the presence of Si dopants considerably increases the energy gain for water chemisorption and decreases the energy barrier for water dissociation by more than 50 %. We provide a physical rational for the phenomenon by analyzing the electronic charge displacements occurring upon adsorption. We also show that once hydroxylated, the surface is able to bind further water molecules much strongly than the clean surface via hydrogen bond networks. This two-step process is consistent with and can explain the enhanced hydrophilic character observed in carbon-based films doped by silicon.

✉ M. C. Righi
mcrighi@unimore.it

Seiji Kajita
fine-controller@mosk.tytlabs.co.jp

[1] Toyota Central R&D Labs., Inc., 41-1, Yokomichi, Nagakute, Aichi 480-1192, Japan

[2] Istituto Nanoscienze, CNR-Consiglio Nazionale delle Ricerche, 41125 Modena, Italy

Keywords Si-doped diamond-like carbon · Tribochemistry · Hydrophilicity · Water adsorption · Ab initio calculations

1 Introduction

Polycrystalline diamond and diamond-like carbon (DLC) provide fully biocompatible, ultra-hard, low-friction, wear-resistant coatings, which make them very attractive for numerous applications ranging from biomedicine to tribology. Recently, a number of studies have been devoted to the incorporation of elements, such as silicon, nitrogen, and metals, into the carbon films to modify their structural and surface properties [1–4]. Silicon, in particular, is incorporated in DLC to improve the adhesion strength on substrates [5, 6], thermal stability [7–10], and biocompatibility [11, 12] and reduce the friction coefficient [13–17].

The microscopic mechanisms that lead to the extremely low friction coefficient of silicon-doped DLC (Si-DLC) are still unclear. It is expected that the presence of Si dopants modifies the surface–water interaction and tribochemistry in humid environments. In fact, silanol groups (Si–OH) have been detected on the surface of as-deposited Si-DLC in ambient air by derivatization X-ray photoelectron spectroscopy [18–20]. This surface termination, resulting from the dissociative adsorption of water molecules, has been suggested to promote the formation of a water boundary layer, which prevents the direct contact of the sliding surfaces and consequently reduces friction [20]. This hypothesis has been confirmed by molecular dynamics (MD) simulations, which showed that water molecules strongly attached to the surface hydroxyl groups via hydrogen bond networks were able to separate the sliding surfaces in shear conditions [21].

A decrease in water contact angle with an increase in Si doping in the DLC coating has been recently reported [22, 23], but the chemical role of the Si dopants has not been elucidated. Understanding the microscopic mechanisms that govern the wettability of doped DLC coatings is of paramount importance not only for tribology, but also for biomedical applications such as contact lens and artificial heart valves [24, 25].

Here, we apply first-principle calculations based on density functional theory (DFT) to investigate the effects of silicon dopants on water adsorption at diamond surfaces. Despite its relevance for lubrication, biological materials application, and microelectronics, the diamond–water interface has been scarcely investigated by ab initio methods [26–29]. The use of a parameter-free approach is particularly important because classical potentials hardly capture the water–surface interaction [30], and chemical reactions such as water dissociation at the surface cannot be accurately described. We consider the diamond (001) surface, which presents a dimer reconstruction composed of carbon double bonds, to resemble the thin DLC layer of sp^2 carbon often detected in tribologial contacts [28]. Silicon atoms are located at substitutional sites identified as most stable at the surface, with a concentration typical for Si-DLC. The simulated crystalline system differs from the amorphous matrix of sp^2 and sp^3 carbon of real Si-DLC coatings [4, 31, 32]; however, it constitutes a minimal model suitable to give insights into the *local* physical–chemical interactions that promote water adsorption and dissociation at the Si sites. By comparing the adsorption energies and dissociation barriers of Si-doped and clean diamond surfaces, we elucidate the chemical role of Si dopants in modifying the hydrophilic character of the carbon-based films.

2 Method

We model the (001) surface with periodic supercells containing a diamond slab reconstructed on both the sides with 10-layer thickness and 4×3 in-plane size. The surface presents a 2×1 reconstruction constituted of dimers that give rise to alternating rows and trenches of sp^2- and sp^3-bonded carbon atoms. A vacuum region of 20 Å thickness is included in the supercell to separate each slab from its periodic replicas along the [001] direction. Silicon atoms are located at substitutional sites, consistently with the experimental observation that silicon atoms in Si-DLC are surrounded by carbon atoms, and not by oxygen or other silicon atoms [31, 32]. A 8.3 % Si concentration is realized, which is consistent with that used in the experiments [33].

Static ab initio DFT calculations are performed by means of the pseudopotential/plane-wave computer code included in the QUANTUM ESPRESSO package [34]. The Perdew, Burke, and Ernzerhof generalized gradient approximation (GGA-PBE) is used for the exchange-correlation functional [35], and all the simulations include the spin polarization. The electronic wave functions are expanded on a plane-wave basis set with a cutoff energy of 25 Ry, and the ionic species are described by ultra-soft pseudopotentials [36]. The k points in the Brilliouin zone are sampled by means of a $2 \times 3 \times 1$ Monkhorst–Pack grid [37]. In the geometry optimization procedure, all the atoms except for those belonging to the slab bottom layer are allowed to relax until the forces become lower than 0.001 Ry/Bohr. The adsorption energy of a water molecule on the surface is calculated as $E_{ad} = E_{tot} - E_{surf} - E_{H_2O}$, where E_{tot}, E_{surf} and E_{H_2O} are the energies of the adsorbate system, the clean surface, and water molecule. E_{tot} and E_{surf} are calculated using the same supercell, while for E_{H_2O}, we use a cubic cell with edge 16 Å long, being the water molecule assumed as isolated. The reaction path and energy barrier for water dissociation are calculated by means of the nudged elastic band (NEB) method within the "climbing the image" scheme [38, 39]. The NEB method is able to identify the minimum energy path (MEP) for the system transition between two stable configurations. In our case, they correspond to water physisorption and dissociative chemisorption configurations, respectively. In the NEB calculations, we reduce the slab thickness to six layers in order to accelerate the convergence of the method.

3 Results and Discussion

3.1 Effects of Silicon Dopants on the Process of Surface Hydroxylation

In order to construct a realistic model for the Si-incorporating C(001) surface, we identify the most favorable location for the silicon atoms by comparing the stability of different substitutional sites. As shown in Fig. 1, the compared sites are located within the first, second, and third surface layers. The configuration containing the Si–C heterodimer (Fig. 1a) turned out to be the most energetically favored. Indeed, Si dopant surrounded by C-sp^2 atoms has been identified as the prevailing configuration in Si-DLC films by nuclear magnetic resonance experiments [31].

As a next step, we evaluate the effects of silicon on the dissociative adsorption of water molecules. The considered adsorption configurations are modeled by positioning the two fragments (−H and −OH) of the dissociated molecule

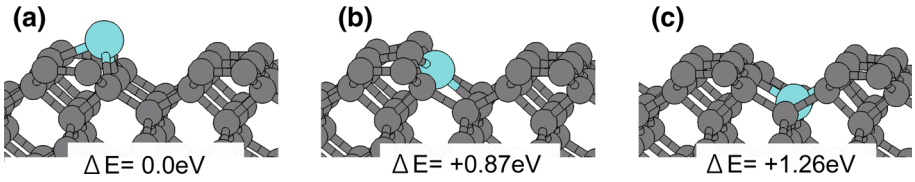

Fig. 1 Relative stability of different substitutional sites for the Si dopant. The energy differences are referred to the most stable configuration (**a**), where the Si atom is located in the first surface layer and forms a Si–C heterodimer. The *gray* and *blue* balls indicate Si and C atoms, respectively (Color figure online)

on different sites. In particular, we model adsorption processes involving either only one dimer or two adjacent dimers (belonging both to the same row or separated by a trench). The optimized configurations and the corresponding adsorption energies are shown in Fig. 2. As can be seen from the first and second rows, where the Si-doped surface is considered, the adsorption configurations containing a Si–OH group are more stable than those containing a Si–H group by more than 1 eV. The comparison between the adsorption energies for Si-doped and undoped surfaces (first and third rows of Fig. 2) indicates that the stability of a Si–OH group is significantly higher than that of a C–OH group by approximately 1.5 eV. On the contrary, the energy gain for hydrogen adsorption is almost independent from the presence of silicon (second and third rows). These results indicate that the Si dopant selectively stabilizes the hydroxyl group.

To better understand the above-described results, we analyze the electronic charge displacements and the projected density of states (PDOS) of hydroxylated surfaces.

The charge displacement, $\Delta\rho$, occurring upon adsorption of an OH fragment on the surface is calculated as $\Delta\rho = \rho_{tot} - \rho_{surf} - \rho_{frag}$, where ρ_{tot}, ρ_{surf} and ρ_{frag} are the electronic density of the adsorbed system, the clean

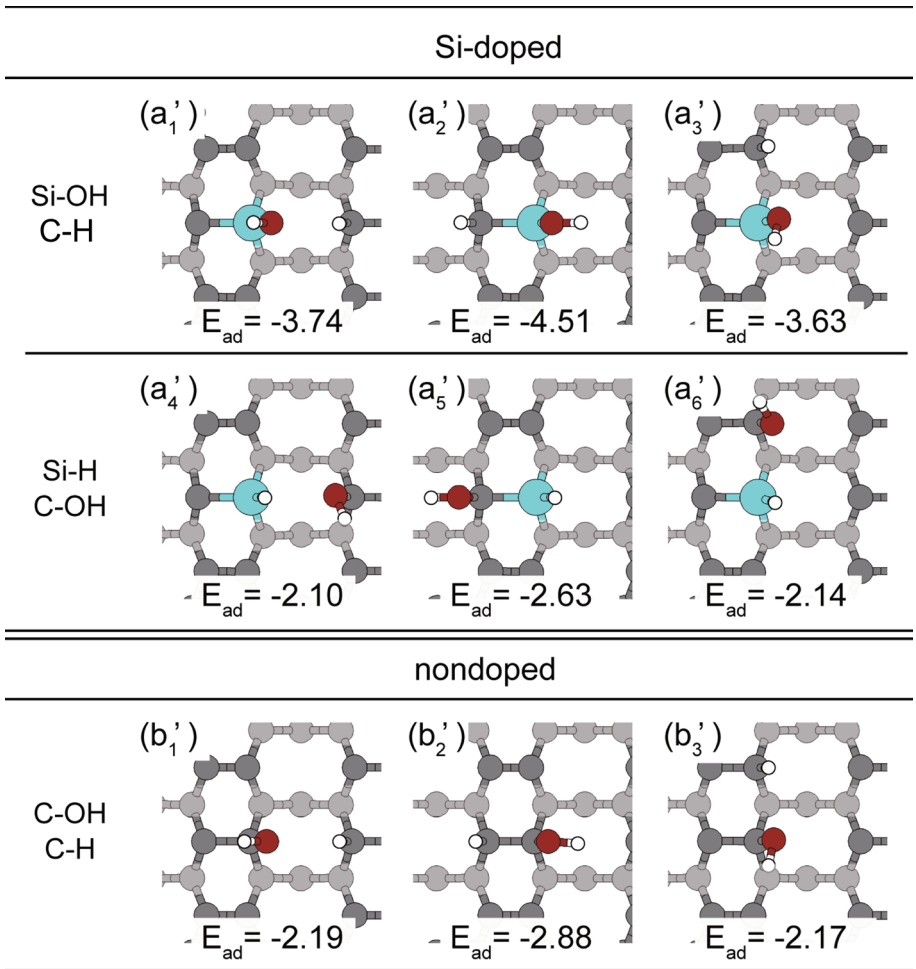

Fig. 2 Dissociative adsorption configurations for a water molecule on the Si-incorporating and clean C(001) surfaces. The adsorptions energies, E_{ad}, are reported in eV. The *red* and *white balls* indicate O and H atoms, respectively (Color figure online)

surface, and isolated fragment. The charge density of the individual components (surface and adsorbate) has been calculated in the geometry that the components have in the composite system. Figure 3 shows the projected charge displacements occurring upon hydroxyl adsorption on the Si-doped (a) and undoped (b) surfaces. The projection of $\Delta\rho$ on the $(\bar{1}10)$ plane is obtained by integration along the perpendicular direction. An accumulation of electrons can be observed both in the O–Si and O–C bond regions, consistently with the covalent character of these bonds. The oxygen bound to the Si site attracts more electrons than the oxygen bound to the C site, as confirmed by the analysis of the Löwdin charges displayed in Fig. 3 [40]. The O–Si bond presents, thus, an ionic character more pronounced than the O–C bond.

To establish a connection between the bonding character and the adsorption energy, we analyze the PDOS for hydroxyl adsorptions shown in Fig. 4. On the clean surfaces, the silicon atom in the heterodimer and the carbon atom in the homodimer (dashed lines) have distinctive peaks below their Fermi energies, at about −0.5 eV. The magnitude of the Si surface state is higher than that of the undoped surface. When a hydroxyl adsorbs on the surface, these surface states disappear because new bonds are formed with the oxygen atom. The occupied surface state of the Si dopant before the adsorption (dashed blue line) shifts above the Fermi energy as empty states (solid blue line), which is an evidence that electrons of the Si dopant transfer to the adsorbed oxygen atom and a bond with enhanced ionic character is formed. Although the electron transfer occurs also in the case of the undoped surface, the oxygen peak of the Si–OH group is located in a lower energy region than that of the C–OH group (red lines). This suggests that the transfer of electrons from the dopant to the oxygen stabilizes the hydroxyl adsorbate. Such enhanced electronic transfer is due to the lower electronegativity of silicon: O (3.44) > C (2.55) > Si (1.90),

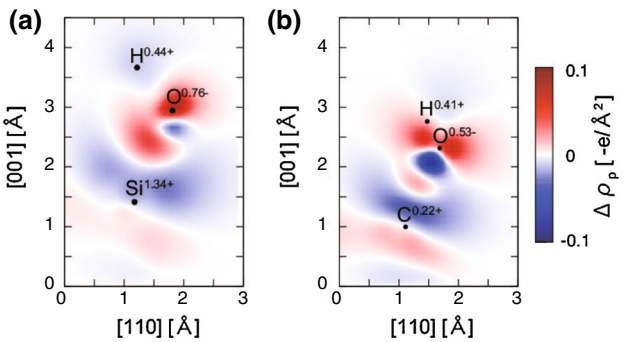

Fig. 3 Charge displacements projected on the $(\bar{1}10)$ plane upon adsorption of OH fragments on the **a** Si-doped and **b** undoped surfaces. The *superscript* of each element indicates the partial charge obtained by the Löwdin charge population analysis

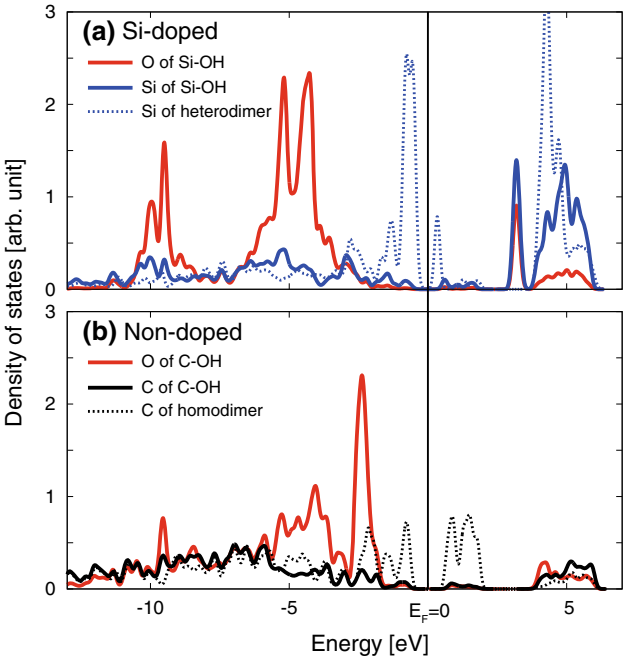

Fig. 4 PDOS of the OH-adsorbed on the **a** Si-doped and **b** undoped surfaces. The origin of the horizontal axis corresponds to the Fermi energy.

where the numbers in the parentheses are the Pauling values [41]. The lower electronegativity of the Si atoms, which are surrounded by carbon atoms in Si-DLC, thus controls the bond polarization and promotes the surface hydroxylation, as shown by the reaction paths described in the following.

We identify the reaction path and energy barrier for water dissociation both on the clean and Si-incorporating C(001) surfaces, by applying the NEB method. As initial states for the reactions, we consider the most favorable configurations for water adsorption shown in Fig. 5a, b.[1] The corresponding final states are chosen among the configurations of Fig. 2. In particular, we consider dissociation both on the trench (a_1', b_1') and on the dimer (a_2', b_2'). In the case of Si-doped surface, the minimum energy path (MEP) identified by the NEB algorithm for the $a \rightarrow a_2'$ transition displays an intermediate minimum corresponding to the a_1' state. This means that one water molecule physisorbed with the geometry of Fig. 5a hardly reacts with only one dimer to form the a_2' configuration. The latter is most likely obtained by the dissociation of more than one molecule.

[1] The latter are identified by comparing the water adsorption energy at different locations. In particular, we sample six positions on a homogeneous grid along the [110] direction centered on the Si atom and covering the heterodimer and half of the sp^3 trench. The in-plane coordinates of the oxygen atom are fixed at the grid point, and all the other degrees of freedom are fully relaxed except for the slab bottom layer

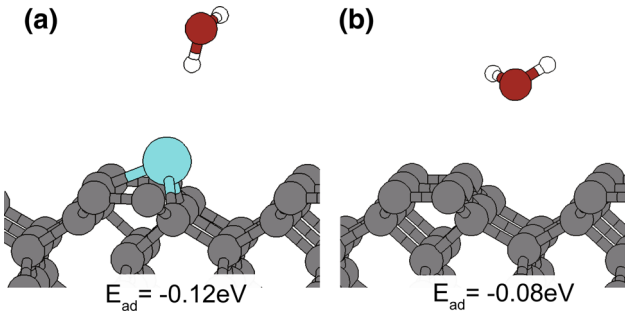

Fig. 5 Most stable configurations identified for molecular adsorption on **a** Si-doped and **b** undoped surfaces

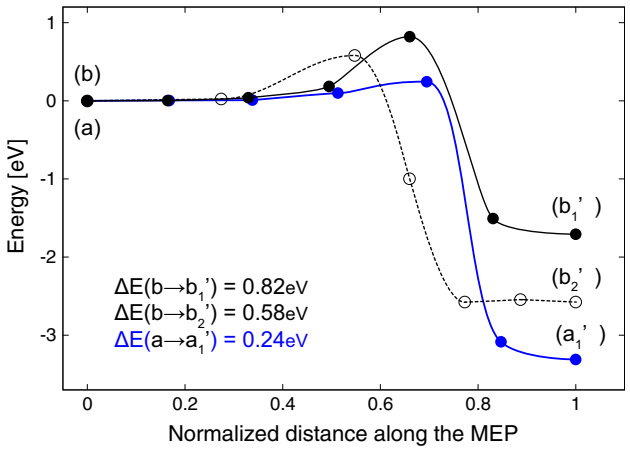

Fig. 6 Reaction paths and the energy barriers ΔE for water dissociations obtained by NEB calculations. The *blue* and *black plots* indicate the NEB images for the Si-doped and undoped surfaces, respectively. The initial (final) states of the reaction paths correspond to the configurations shown in Fig. 5 (Fig. 2), which are labeled in the same way

Figure 6 summarized the results obtained for the reaction paths and energy barriers for water dissociation on the Si-doped surface (blue line) and the undoped surface (black lines). In the latter case, the comparison between the results obtained for the $b \rightarrow b_1'$ and $b \rightarrow b_2'$ transitions indicates that water dissociation occurs most likely within the dimer row rather than within the trench, in agreement with previous calculations [27]. The comparison between the $a \rightarrow a_1'$ and $b \rightarrow b_2'$ paths reveals that the Si dopant reduces the energy barrier for the water dissociation by more than 50 %. This significant reduction in the reaction barrier is caused by the stabilization of the hydroxylated configuration by the Si dopant. The reaction energy associated with the $a \rightarrow a_1'$ transition is, in fact, 0.75 eV higher than the reaction energy of the $b \rightarrow b_2'$ transition.

3.2 Effects of Surface Hydroxylation on Water Adsorption

As last step in our analysis, we clarify the effects of surface hydroxylation on the physisorption of further water molecules, i.e., on the surface wettability. We focus on the effects of hydroxylation because several studies have highlighted the important role of −OH groups in enhancing the surface hydrophilicity and frictional performances [17–20, 25]. Moreover, according to the phase diagram of the C(001) surface that we presented in a previous work [42], the full hydroxyl termination is more favorable than the termination containing both −OH and −H adsorbates, for a wide range of the oxygen and hydrogen chemical potentials and especially when the condition $2\mu_H + \mu_O = \mu_{H_2O}$ is satisfied, i.e., when the adsorbates are in thermodynamic equilibrium with water vapor. We compare the energy for molecular adsorption on OH-terminated, H-terminated, and clean surfaces. In the first case, we consider both Si-doped and undoped surfaces. The calculated adsorption energies, which are reported in Figs. 5 and 7, indicate that the surface hydroxylation highly enhances water attraction: The physisorption energy in the presence of adsorbed hydroxyl groups is three times higher than in the absence. Furthermore, the distance between the physisorbed molecule on the hydroxylated surface (calculated as the distance between the O atom of the physisorbed molecule and the H atom of the adsorbed −OH group) ia of about 1.8 Å. This value is lower than that obtained for the hydrogenated surface of Fig. 7c and is very close to 1.9 Å, which is the typical length of hydrogen bonds in bulk water. These results indicate that the surface hydroxylation enhances the attraction of water molecules toward the surface thanks to the formation of hydrogen bond networks that involve the

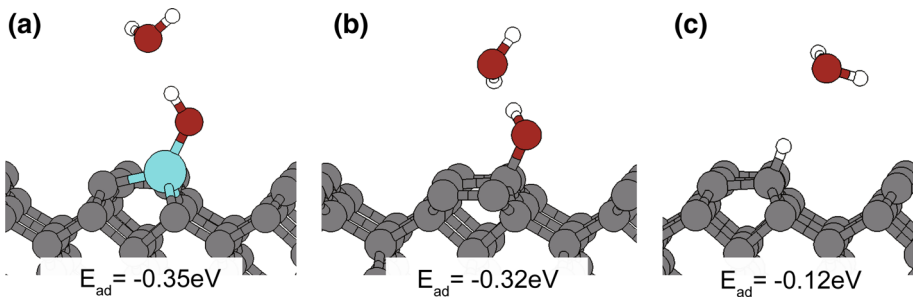

Fig. 7 Water physisorption at OH- and H-terminated surface sites. In the first case, both Si-doped and undoped surfaces are considered

chemisorbed −OH groups. This increases the diamond/DLC hydrophilicity.

It should be kept in mind that the GGA functional in DFT fails in the exact prediction of adsorption energies because of the inadequate description of the van der Waals (VdW) interactions [27, 43–45]. However, the qualitative conclusions derived from this study should hold on the basis of a comparative analysis of the result present in the literature: In our previous DFT study, the energies for water physisorption and dissociation on the diamond surface were calculated both with and without the inclusion of VdW interactions. The results indicate that VdW inclusion increases the water physisorption energy approximately by 0.1 eV on average and decreases the energy barrier for water dissociation by 30 % [27]. Even if we take into account of the errors maximally, the conclusions on the effects of Si dopants here derived will not be altered because they are based on estimated energy differences that are much higher than these errors.

Finally, by comparing the adsorption energies reported in Fig. 7a, b, we observe that water adsorption on hydroxylated surfaces is not significantly affected by the presence of Si dopants. Therefore, the main effect of Si dopants is to favor water dissociation. The consequent hydroxyl termination enhances the hydrophilic character of the surface.

4 Conclusions

To shed light into the effects of Si dopants in increasing the hydrophilicity of carbon-based coatings, we study the interaction of water molecules with Si-doped and undoped C(001) surfaces by means of ab initio calculations. We find that the energy gain for water dissociative adsorption increases by approximately 1.5 times in the presence of substitutional Si atoms at the surface. The analysis of the electronic charge displacements occurring upon adsorption reveals that this stabilization effect is due to the larger polarization of Si–OH bonds with respect to C–OH bonds. We apply the NEB method to identify the reaction paths for water dissociation and find that the energy barrier on the Si-incorporating surface is 50 % lower than on the clean surface. The process of surface hydroxylation is, thus, highly favored by Si dopants.

Once hydroxylated, the surface is able to attract further water molecules more strongly than the clean surface by hydrogen bond formation (the energy is more than three times higher on the OH-terminated surface than on the clean surface). This two-step tribochemical process is consistent with and can explain the enhancements of hydrophilic character and the consequent friction reduction observed in carbon films doped by silicon.

Acknowledgments We acknowledge the CINECA consortium for the availability of high-performance computing resources and support through the ISCRA-B TRIBOGMD project.

References

1. Sanchez-Lopez, J.C., Fernandez, A.: Doping and alloying effects on DLC coatings. In: Donnet, C., Erdemir, A. (eds.) Tribology of diamond-like carbon films, pp. 311–338. Springer, New York (2008)
2. Bewilogua, K., Hofmann, D.: History of diamond-like carbon films—from first experiments to worldwide applications. Surf. Coat. Technol. **242**, 214–225 (2014)
3. Donnet, C.: Recent progress on the tribology of doped diamond-like and carbon alloy coatings: a review. Surf. Coat. Technol. **100–101**, 180–186 (1998)
4. Grill, A.: Diamond-like carbon: state of the art. Diam. Relat. Mater. **8**, 428–434 (1999)
5. Mori, H., Tachikawa, H.: Increased adhesion of diamond-like carbon–Si coatings and its tribological properties. Surf. Coat. Technol. **149**, 224–229 (2002)
6. Miyake, S., Kaneko, R., Kikuya, Y., Sugimoto, I.: Micro-tribological studies on fluorinated carbon films. ASME J. Tribol. Trans. **113**, 384–389 (1991)
7. Camargo Jr, S.S., Santos, R.A., Neto, A.L.B., Carius, R., Finger, F.: Structural modifcations and temperature stability of silicon incorporated diamond-like a-C: H films. Thin Solid Films **332**, 130–135 (1998)
8. Wu, W.J., Hon, M.H.: Thermal stability of diamond-like carbon films with added silicon. Surf. Coat. Technol. **111**, 134–140 (1999)
9. Varma, A., Palshin, V., Meletis, E.I.: Structure-property relationship of Si-DLC films. Surf. Coat. Technol. **148**, 305–14 (2001)
10. Hatada, R., Flege, S., Baba, K., Ensinger, W., Kleebe, H.-J., Sethmann, I., Lauterbach, S.: Temperature dependent properties of silicon containing diamondlike carbon films prepared by plasma source ion implantation. J. Appl. Phys. **107**, 083307 (2010)
11. Zhao, Q., Liu, Y., Wang, C., Wang, S.: Bacterial adhesion on silicon-doped diamond-like carbon films. Diam. Relat. Mater. **16**, 1682–1687 (2007)
12. Bendavid, A., Martin, P.J., Comte, C., Preston, E.W., Haq, A.J., MagdonIsmail, F.S., Singh, R.K.: The mechanical and biocompatibility properties of DLC-Si films prepared by pulsed DC plasma activated chemical vapor deposition. Diam. Relat. Mater. **16**, 1616–1622 (2007)
13. Oguri, K., Arai, T.: Friction coefficient of Si–C, Ti–C and Ge–C coatings with excess carbon formed by plasma-assisted chemical vapour deposition. Thin Solid Films **208**, 158–160 (1992)
14. Kim, M.G., Lee, K.R., Eun, K.Y.: Tribological behavior of silicon-incorporated diamond-like carbon films. Surf. Coat. Technol. **112**, 204–209 (1999)
15. Ikeyama, M., Nakao, S., Miyagawa, Y., Miyagawa, S.: Effects of Si content in DLC films on their friction and wear properties. Surf. Coat. Technol. **191**, 38–42 (2005)
16. Lanigan, J., Zhao, H., Morina, A., Neville, A.: Tribochemistry of silicon and oxygen doped, hydrogenated Diamond-like Carbon in fully-formulated oil against low additive oil. Tribol. Int. **82**, 431–442 (2015)
17. Wu, X., Ohana, T., Tanaka, A., Kubo, T., Nanao, H., Minami, I., Mori, S.: Tribochemical reaction of Si-DLC coating in water studied by stable isotopic tracer. Diam. Relat. Mater. **17**, 147–153 (2008)

18. Takahashi, N.: Analysis of silanol by derivatization XPS. R&D Rev. Toyota CRDL **41**, 52 (2006)
19. Mori, H., Takahashi, N., Kazuyuki, N., Tachikawa, H., Ohmori, T.: Low friction property and its mechanism of DLC-Si films under dry sliding conditions. SAE Int. **07M–426**, 16 (2007)
20. Kato, N., Mori, H., Takahashi, N.: Spectroscopic ellipsometry of silicon-containing diamond-like carbon (DLC-Si) films. Phys. Stat. sol. **5**, 1117–1120 (2008)
21. Washizu, H., Sand, S., Hyodo, S., Ohmori, T., Nishino, N., Suzuki, A.: Molecular dynamics simulations of elasto-hydrodynamic lubrication and boundary lubrication for automotive tribology. J. Phys.: Conf. Ser. **89**, 012009 (2007)
22. Dearnaley, G., Arps, J.H.: Biomedical applications of diamond-like carbon (DLC) coatings: a review. Surf. Coat. Technol. **200**, 2518–2524 (2005)
23. Saitoa, T., Hasebea, T., Yohenaa, S., Matsuokaa, Y., Kamijoc, A., Takahashic, K., Suzukia, T.: Antithrombogenicity of fluorinated diamond-like carbon films. Diam. Relat. Mater. **14**, 1116–1119 (2005)
24. Borisenko, K.B., Reavy, H.J., Zhao, Q., Abel, E.W., Biomed, J.: Adhesion of protein residues to substituted (111) diamond surfaces: an insight from density functional theory and classical molecular dynamics simulations. Mater. Res. A **86**, 1113–1121 (2008)
25. Yi, J.W., Moon, M.W., Ahmed, S.F., et al.: Long-lasting hydrophilicity on nanostructured Si-incorporated diamond-like carbon films. Langmuir **26**, 17203–17209 (2010)
26. Okamoto, Y.: Initial H_2O-induced oxidation of C(001)-(21): a study with hybrid density-functional theory. Phys. Rev. B **58**, 6760 (1998)
27. Manelli, O., Corni, S., Righi, M.C.: Water adsorption on native and hydrogenated diamond (001) surfaces. J. Phys. Chem. C **114**, 7045–7053 (2010)
28. Bouchet, M.-I.B., Zilibotti, G., Matta, C., Righi, M.C., Vandenbulcke, L., Vacher, B., Martin, J.-M.: Friction of diamond in the presence of water vapor and hydrogen gas. coupling gas-phase lubrication and first-principles studies. J. Phys. Chem. C **116**, 69666972 (2012)
29. Zilibotti, G., Corni, S., Righi, M.C.: Load-induced confinement activates diamond lubrication by water. Phys. Rev. Lett. **111**, 146101 (2013)
30. Grossman, J.C., Schwegler, E., Galli, G.: Quantum and classical molecular dynamics simulations of hydrophobic hydration structure around small solutes. J. Phys. Chem. B **108**, 15865–15872 (2004)
31. Iseki, T., Mori, H., Hasegawa, H., Tachikawa, H., Nakanishi, K.: Structural analysis of Si-containing diamond-like carbon. Diam. Relat. Mater. **15**, 1004–1010 (2006)
32. Palshin, V., Tittsworth, R.C., Fountzoulas, C.G., Meletis, E.I.: X-ray absorption spectroscopy, simulation and modeling of Si-DLC films. J. Mater. Sci. **37**, 1535–1539 (2002)
33. Nakanishi, N., Mori, H., Tachikawa, H., Itou, K., Fujioka, M., Funaki, Y.: Investigation of DLC-Si coatings in large-scale production using DC-PACVD equipment. Surf. Coat. Technol. **200**, 4277–4281 (2006)
34. Giannozzi, P., et al.: QUANTUM ESPRESSO: a modular and open-source software project for quantum simulations of materials. J. Phys.: Condens. Matter **21**, 395502 (2009)
35. Perdew, J.P., Burke, K., Ernzerhof, M.: Generalized gradient approximation made simple. Phys. Rev. Lett. **77**, 3865 (1996)
36. Vanderbilt, D.: Soft self-consistent pseudopotentials in a generalized eigenvalue formalism. Phys. Rev. B **41**, 7892(R) (1990)
37. Monkhorst, H.J., Pack, J.D.: Special points for Brillouin-zone integrations. Phys. Rev. B **13**, 5188 (1976)
38. Henkelman, G., Jonsson, H.: Improved tangent estimate in the nudged elastic band method for finding minimum energy paths and saddle points. J. Chem. Phys. **113**, 9978–9985 (2000)
39. Henkelman, G., Uberuaga, B.P., Jonsson, H.: A climbing image nudged elastic band method for finding saddle points and minimum energy paths. J. Chem. Phys. **113**, 9901–9904 (2000)
40. Löwdin, P.O.: On the non-orthogonality problem connected with the use of atomic wave functions in the theory of molecules and crystals. J. Chem. Phys. **18**, 365–375 (1950)
41. Lide, D.R.: Handbook of chemistry and physics. CRC Press, Boca Raton (2002)
42. Zilibotti, G., Righi, M.C., Ferrario, M.: Ab initio study on the surface chemistry and nanotribological properties of passivated diamond surfaces. Phys. Rev. B **79**, 075420 (2009)
43. Kajita, S., Minato, T., Kato, H.S., Kawai, M., Nakayama, T.: First-principles calculations of hydrogen diffusion on rutile TiO_2(110) surfaces. J. Chem. Phys. **127**, 104709 (2007)
44. Sprik, M.: Ab initio molecular dynamics simulation of liquids and solutions. J. Phys.: Condens. Matter **8**, 9405–9409 (1996)
45. Johnson, E.R., DiLabio, G.A.: Structure and binding energies in van der Waals dimers: comparison between density functional theory and correlated ab initio methods. Chem. Phys. Lett. **419**, 333–339 (2006)